encit 2022

ABCM Associação Brasileira de Engenharia e Ciências Mecânicas

19th Brazilian Congress of Thermal Sciences and Engineering
November 06th-10th, 2022, Bento Gonçalves - RS - Brazil

# ENC-2022-0122
# INFLUENCE OF GROOVES ON THE THERMAL BEHAVIOR OF MINI PULSATING HEAT PIPES

**Larissa Krambeck**
**Kelvin Guessi Domiciano**
**Marcia Barbosa Henriques Mantelli**
Department of Mechanical Engineering, Federal University of Santa Catarina, Florianopolis/SC, 88040-900, Brazil
larissa.krambeck@labtucal.ufsc.br; kelvin.guessi@labtucal.ufsc.br; marcia@labtucal.ufsc.br

***Abstract.*** *This research experimentally investigated the impact of grooves on the thermal performance of mini flat pulsating heat pipes used for surface electronic cooling applications. A novel channel design, which was made of a square channel with 4 (four) machined grooves along the longitudinal direction, was proposed, combining characteristics of an oscillating heat pipe and capillary structure. Three PHPs with 16 parallel channels were manufactured using diffusion bonding, tested and compared to each other. PHP-A had a conventional square channel. PHP-B and PHP-C were fabricated with the novel channel profile. Their essential difference is that PHP-C has grooves through all sections while PHP-B presents the novel design only in the evaporator section. Ethanol was used as the working fluid. Heat transfer rates from 10 to 170 W were studied under horizontal and gravity-assisted orientations. Both PHPs with the novel channel reduced the thermal resistance and anticipated the startup in the gravity-assisted orientation. However, the modifications only in the evaporator showed to be a better alternative for electronics cooling submitted a wide range of dissipated power. Without gravity assistance, just the square PHP operated satisfactorily, being the best option under concentrated thermal loads. Although the 4 (four) machined grooves and the edges worked as a capillary structure, the promoted capillarity was not enough for a proper operation in the horizontal position.*

***Keywords:*** *pulsating heat pipe, grooves, thermal performance, electronics cooling.*

## 1. INTRODUCTION

Passive heat transfer devices have exhibited a better alternative than the active ones in electronics cooling due to technical simplicity, high reliability and low cost. Two-phase mini heat exchangers are among the most advanced technologies for the thermal management of electronics, including those for space applications such as microsatellites (Baturkin, 2005).

The pulsating heat pipe (PHP), also known as oscillating heat pipe, has deserved special attention in recent literature. This technology is formed by curved channels partially filled with a working fluid that moves in an oscillatory or pulsating cycle, transferring heat efficiently. Instead of a capillary structure that promotes liquid circulation in conventional heat pipes, the PHPs use confined channels to displace the liquid. Else, sensible heat transports most of the heat. Due to these characteristics, the PHPs can carry high heat fluxes, up to 300 W/cm$^2$, and is able to collect heat at hard-to-reach hot spots in real applications (Laun et al., 2015; Taft et al., 2012; Zhang and Faghri, 2008).

A PHP is essentially composed of three regions: evaporator that receives the heat to be transported, adiabatic section and condenser that removes the heat, as shown schematically in Figure 1. A temperature gradient between the evaporator and the condenser is needed as the minimum condition for the PHP to begin operation in a working fluid oscillating mode, once it creates a pressure difference between the hot and the cold side, promoting its movement (Zhang and Faghri, 2008).

Flat plates are alternatives to PHPs, where the channels that the working fluid flows are internal to a thin plate, which can be a few millimeters thick. They have great potential as a cooling alternative for electronic gadgets, as they are easy to integrate into the heat source and able to transfer high and concentrate thermal loads (Winkler et al., 2020)

Besides the large heat transfer ability, several researchers have performed strategies in recent years to improve further the thermal behavior PHPs. These efforts involve the study of different working fluids, such as binary and nanofluids, physical properties and surface finishing of internal surfaces, and channel geometries, including the cross-section geometry, which can directly impact the working fluid flow patterns arrangement inside the channels (Qu et al., 2017).

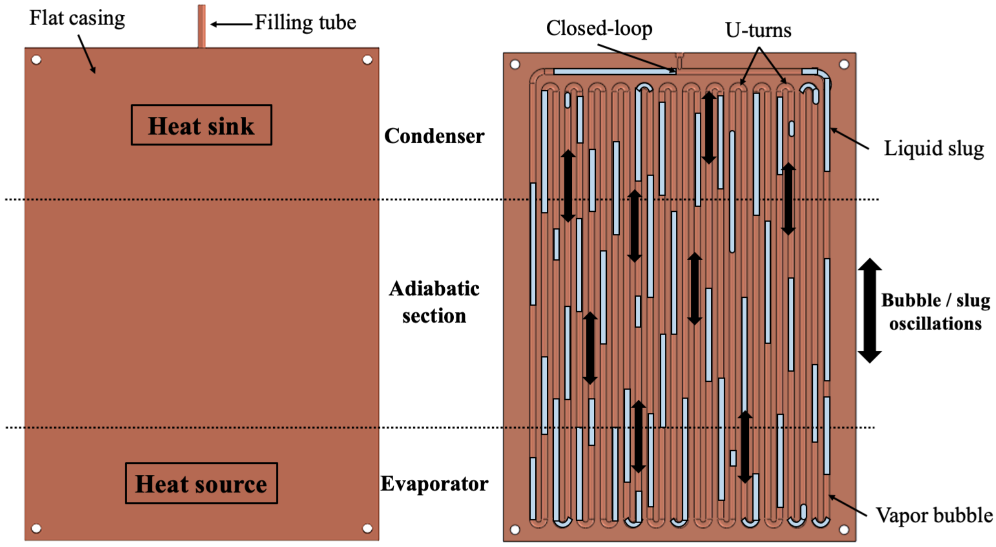


Figure 1. Operating principle of a closed-loop flat plate PHP.

Square and round channels are the most common PHP cross-section geometries in the literature, as they are easy to manufacture. Among them, the square channel PHP presents lower thermal resistances, lower evaporator temperatures and the ability to withstand higher heat loads. These are the benefits of the corners in rectangular profiles that accumulate liquid, acting as capillary structures and keeping the evaporator wet. Also, the edges decrease the Kelvin-Helmholtz instabilities and facilitate reaching the annular flow that improves the PHP thermal behavior. As a negative point, the square channels usually show a delay in the operation startup, as they require a higher temperature difference to start (Khandekar et al., 2003; Krambeck et al., 2022; Yang et al., 2009).

Some authors have studied different cross-section geometries with sharp angles in PHPs. Qu et al. (2007) concluded that a sharper angle of the triangular channel improved the capillary force and heat transfer mechanism. Cai et al. (2006) created microgrooves in a tubular PHP that made the evaporator temperature more homogenous. Qu et al. (2017) improved the effective thermal conductivity of a tubular PHP by internal helical microgrooves. In flat plate PHPs, high quality lateral sharp grooves in round cross-section channels were studied by Krambeck et al. (2022), concluding that the thermal resistance decreased.

Despite the large number of researches involving the high thermal efficiency of PHPs to transport heat in electronics cooling and techniques to improve their thermal performance, several authors still use dimensions and geometries that are incompatible with these applications. For example, Yang et al. (2009) studied PHPs with 180 x 120 mm$^2$ and Mameli et al. (2014) tested tubular PHPs totalizing 203.5 x 186 mm$^2$ under varying conditions. Power electronics require a cooling device that is the most simple, flat, small, and compact as possible (Winkler et al., 2020).

However, the literature does not present studies to enhance PHPs with square cross-section channel geometries. In the present work, the study of the influence of grooves on the thermal performance of mini flat PHPs with square channels was performed experimentally. A novel channel design was proposed, composed of a square channel with 4 (four) grooves along the longitudinal direction, combining characteristics of a mini oscillating heat pipe and mini heat pipes due to the grooved capillary structure. The thermal characteristics of a similar flat plate PHP with simple square channels were also studied, so that the effect of grooves in the performance of PHP with square geometry can be addressed. The studied PHPs are thin and small, so they can be considered for electronic cooling applications.

## 2. MINI FLAT PULSATING HEAT PIPES

Three closed-loop flat plate PHPs of 8 U-turns, which correspond to 16 interconnected parallel channels, of 100 x 55 x 2.5 mm$^3$, were manufactured. The difference among them is in the cross-section geometry of the channels. PHP-A has a conventional square channel. PHP-B and PHP-C were fabricated with square channels with grooves. While PHP-C has grooves along all three sections, the grooves in PHP-B are present only in the evaporator section. These channel geometries are shown in Figure 2.

The devices were divided into an evaporator of 14 mm, an adiabatic section of 71 mm and a condenser of 15 mm (total length of 100 mm). Ethanol was the working fluid. The internal volume of PHP-A, PHP-B and PHP-C were 2.68, 3.00 and 3.10 ml, respectively.

## 2.1 Diffusion bonding of the PHPs

The diffusion bonding technique was used for the fabrication of the tested devices. It basically consists of piling previously machined plates and bonding them in special furnaces that provide a controlled atmosphere (including high vacuum), high temperatures and a hydraulic system able to apply pressure to the stack.

After machined and piled, the plate positions within the stack were guaranteed by spot welding. The diffusion bonding furnace *PVA-Tepla*™, available at Heat Pipe Laboratory (Labtucal/UFSC), was set at a temperature of 875 °C and to a pressure of 3.5 MPa. The plate stack was kept in these conditions for 6400 s. Once the bonding cycle was complete, the furnace was cooled down to the ambient temperature. The heating and cooling processes were carried out in a high vacuum atmosphere, better than 5 x $10^{-6}$ mbar. Once the bonding cycle was complete, rapid cooling was promoted by argon, breaking the high vacuum.

To finalize the manufacturing process, a capillary tube, used for charging the devices with the working fluid, was brazed to the PHPs. A leak test was performed on all testes devices by means of a helium leak detector (*Edwards Spectron*™ 5000 Helium).

## 2.2 PHP plate geometries

Basically, the PHPs are composed of two flat non-machined cover plates and one or two internal machined plates, depending on the channel geometry desired. These plate geometries are illustrated in Figure 2 and described in the sequence.

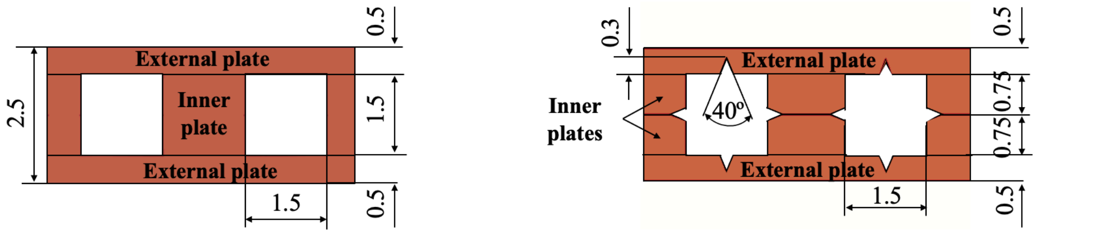


a) PHP-A: square channel b) PHP-B and PHP-C: square channel with grooves

Figure 2. Channel geometries of the PHPs [mm].

### 2.2.1 PHP-A: square channels

The external plates of the tested PHPs have 0.5 mm thickness. The square cross-section channel (PHP-A) is formed by two external plates and an inner plate of 1.5 mm in thickness, with rectangular cross-section channels, machined using a water-jet cutting machine with 1.5 mm in width, as detailed in Figure 2a. All pieces were cleaned with acetone and sulfuric acid. After the cleaning, the plates are carefully piled and kept at the fixed positions among themselves by spot welding, as presented in Figure 3, guaranteeing the desired square geometry in the final PHP. After that, the device was located in the furnace.

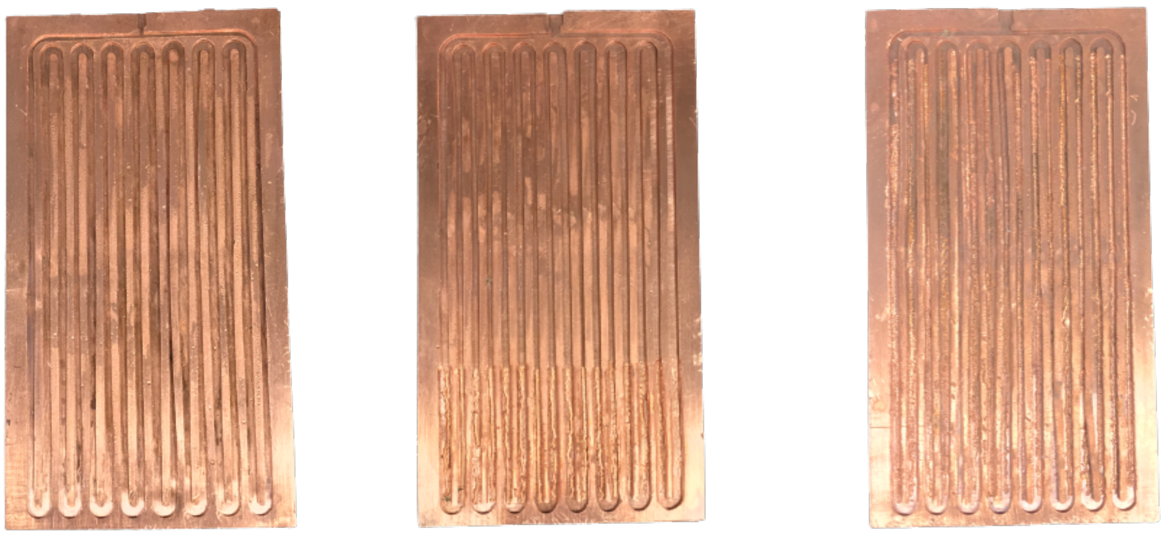

a) PHP-A b) PHP-B: grooves in the evaporator c) PHP-C: grooves along three sections

Figure 3. PHP-A, PHP-B and PHP-C before the diffusion bonding.

### 2.2.2 PHP-B and PHP-C: square channels with grooves

For these PHPs, the same procedure described in the last section was adopted, however, instead of one inner plate of 1.5 mm thick, two plates of 0.75 mm were used and piled, with the same groove geometry of PHP-A. Besides, small chamfers were machined at the corner of channels, so that, when stacked, sharp grooves are formed in the channel lateral walls. To provide two more grooves to the channels, notches were engraved in the channel area of both external plates (see Fig. 2b). These chamfers and notches were provided just in the evaporator for PHP-B and along all the sections for PHP-C, as shown in Figure 3.

## 2.3 Resulting channel profiles

Figure 4 shows a picture of the resulting square cross-section of PHP-A, after the diffusion bonding. The desired shape and the dimensions were maintained. The geometry of the grooves that resulted from the fabrication process was harmed due to their small size, as shown in Fig. 5. The high pressures applied during the manufacturing process caused lateral sliding of the inner plates, modifying significantly the channel shapes, as detailed in Fig. 5b. However, besides being different from the expected geometry, the created grooves can retain liquid, promoting capillarity and so affecting the PHP thermal performance.

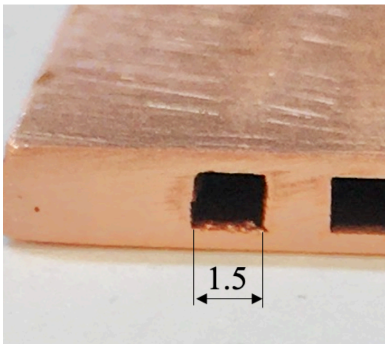


Figure 4. Geometry of the square channel [mm].

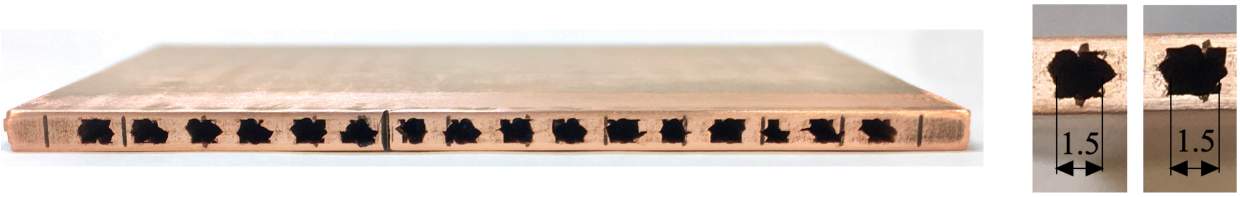


a) cross-sectional view of the channels b) detailed view

Figure 5. Geometry of the fabricated square-grooved channel [mm].

## 3. EXPERIMENTAL ANALYSIS

## 3.1 Experimental setup

An experimental bench was designed and manufactured to evaluate the thermal performance of the PHPs, subjected to incremental power inputs. A cartridge-type thermal resistor embedded in a copper block (14 x 55 x 15 mm$^3$) was used over the evaporator, to simulate the electronics heat to be transferred. A hollow aluminum block (15 x 55 x 22 mm$^3$), within which cooling water from a thermal bath (*Lauda Proline*™ RP1845) flow, was used to reject heat from the condenser section. A programmable power supply unit (*TDK-Lambda*™ GEN300-17) fed the cartridge heater. The heater and heat sink were distributed on the same side of the PHPs, totalizing a contact area of 770 mm$^2$ in the evaporator and 825 mm$^2$ in the condenser. The contact resistances between the cooler and heater and the PHPs were reduced by thermal grease. An *Isoglas*™ blanket with a thickness of 30 mm was used to insulate the experimental setup. Ten T-type thermocouples (*Omega Engineering*™) monitored the temperatures, which were acquired by a data acquisition system (*DAQ-NI*™ SCXI-1000), stored on a laptop (*Dell*™) and controlled by software (*Labview*™). Nine thermocouples were attached to the external surface by a thermosensitive adhesive strip (*Kapton*™) on the opposite side of the heat source. One thermocouple measured the ambient temperature ($T_{amb}$). Figure 6 presents a sketch of the experimental setup and thermocouple distributions.

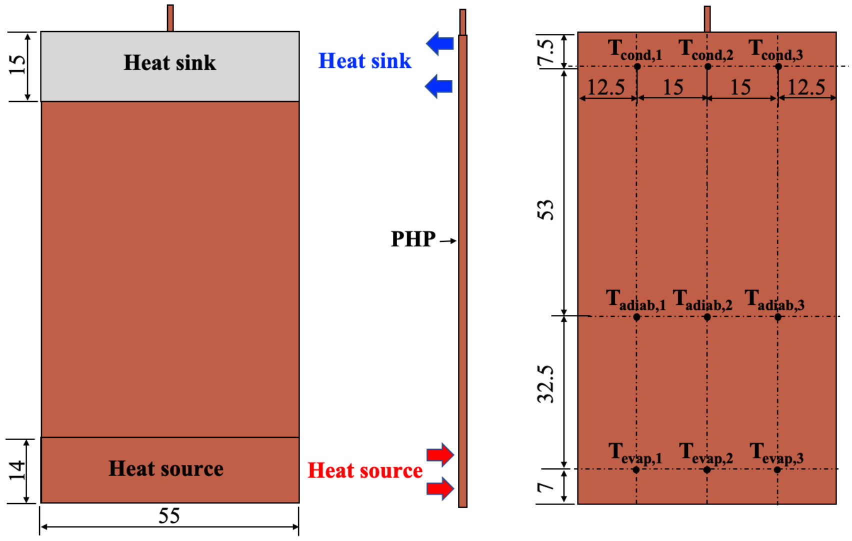


Figure 6. Sketch of the experimental setup and thermocouple distributions [mm].

### 3.2 Experimental procedure

Before any measurement, the tested device was charged with the working fluid. First, the vacuum was provided by means of a compact turbomolecular pumping station (*Edwards*™ T-Station 85). After the vacuum was established, the heat transfer devices were filled with the desired volume of ethanol, using the assistance of a forceps and a Tygon tube. After being charged, the PHPs passed through a purging process to remove any non-condensed gases that might be present, using a variation of the procedure described by Cisterna et al. (2020). The tested volumes of working fluid varied for each PHP, covering a wide range between 5% and 80% of the total internal volume. Also, PHPs with no working fluid were tested under the same conditions to evaluate the heat transportation only by conduction heat transfer. The idea is to test the thermal behavior of the PHPs with different volumes of working fluid to determine the best configuration for each PHP. Heat transfer rates from 10 to 170 W (which correspond to heat fluxes from 1.3 to 22.1 W/cm$^2$) were maintained for 600 s, ensuring the steady-state operation, until the highest, but still safe, operating temperature of electronics was reached, i.e., 100 ° C. The heat flux was defined as the quotient between the dissipated thermal load and the heater contact area.

Tests were performed under horizontal and gravity-assisted (condenser above evaporator) orientations. The cooling water was kept at 20 °C during all the experiments. Experimental data were recorded at a rate of 1 acquisition/second. In the sequence, the PHP-A, PHP-B and PHP-C in their best thermal performance, were compared among themselves, in order to establish the influence of the grooves in the thermal behavior.

### 3.3 Data reduction and uncertainty analysis

The heat transfer performance of heat pipes, including the PHP, can be analyzed using the overall thermal resistance parameter, $R$, defined by:

$$R = \frac{\overline{T}_{evap} - \overline{T}_{cond}}{q} \tag{1}$$

where $\overline{\mathrm{T}}_{\mathrm{evap}}$ and $\overline{\mathrm{T}}_{\mathrm{cond}}$ are the average temperatures of the evaporator and condenser, respectively. The $q$ is the thermal load provided by the power supply unit, calculated by the voltage multiplied by the electric current applied at the cartridge electrical resistor. According to the measurements, the heat leakage to the environment corresponded to less than 1 % of the total thermal load $q$. Thus, heat loss was neglected.

The error propagation technique was used to estimate the experimental uncertainties (Holman, 2011). The uncertainties are derived from the thermocouples, the data acquisition system and the power supply unit. For this, the thermocouples were calibrated using the same experimental setup of the thermal tests. Thus, the temperature uncertainty was approximately ± 0.23 °C. According to the power unit manufacturer, the voltage and current uncertainties were 0.03 V and 0.0085 A, respectively. The maximum uncertainty of the thermal resistance was 0.47 °C/W at 10 W, decreasing to less than 0.02 °C/W at 150 W. The thermal resistance uncertainties are shown by vertical error bars in the graphs.

## 4. RESULTS AND DISCUSSION

### 4.1 Filling volume analysis

The overall thermal resistance is a standard method used to evaluate the heat transfer capacity of PHPs. Smaller thermal resistances demonstrate better thermal performance. The overall thermal resistance of the three empty PHPs (only conduction heat transfer) was R = 1.40 ± 0.23 ºC/W.

The thermal resistances for PHP-C as a function of the thermal load, in steady-state conditions, for gravity-assisted and horizontal positions considering all tested volumes of ethanol are presented in Figure 7.

In the gravity-assisted orientation, the PHPs with all the tested working fluid volumes were able to start their operation from the first power input levels. However, the charging volumes deeply affected the thermal behavior of the device. The PHP-C filled with 0.94, 1.20 ml and 1.50 ml of working fluid presented the lower thermal resistances, reaching the minimum of 0.18 °C/W. For 0.94 ml, the device reached the lowest thermal resistance for 30 W (3.9 W/cm²), and it was able to transfer up to 90 W (11.7 W/cm²) when the evaporator dried out. The PHP-C filled with 1.20 ml of working fluid worked well from 20 W, but the thermal resistance increased when the heat reached 60 W. For the working fluid volume of 1.50 ml, a larger thermal resistance of 0.30 °C/W was reached between 30 and 70 W (3.9 and 9.1 W/cm²). However, the device was able to transfer a maximum power of 120 W (15.6 W/cm²). Therefore, 1.50 ml was chosen as the amount of working fluid that provided the best thermal performance for the device operating in gravity-assisted mode.

In the horizontal orientation (see Figure 7b), PHP-C neither reached the minimal conditions to initiate a PHP operation, nor the grooves were able to return liquid to the evaporator in a typical heat pipe operation. All the tested amounts of working fluid stayed with thermal resistances approximately the same as the empty PHP.

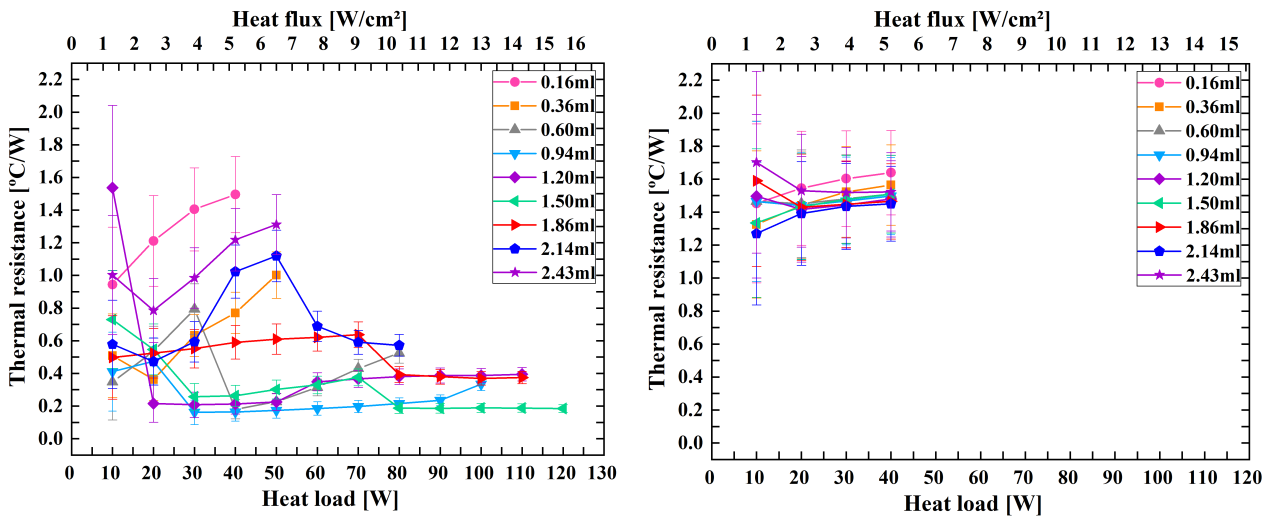


a) gravity-assisted orientation

b) horizontal orientation

Figure 7. Comparison between filling volumes of PHP-C (with grooves in entire channels) by thermal resistances.

As for PHP-C, the charging working fluid volume analysis was performed for PHP-A and PHP-B. Similar analysis and conclusions were achieved for these cases. For the sake of conciseness, the PHPs operating at their best configuration of each PHP are analyzed in the next section. In vertical orientation, the best thermal behavior for PHP-A was accomplished with 1.09 ml of working fluid and, for PHP-B, with 1.20 ml. In horizontal operation mode, PHP-A showed that 1.60 ml was the better volume of working fluid, while, for PHP-B, it was 1.50 ml.

### 4.2 Influence of the grooves on the thermal performance

After the best configuration establishment of each PHP, the impact of grooves on the PHP thermal performance could be investigated. The main distinctions promoted by the grooves were related to the startup and working fluid flow pattern. The transient behavior of three PHPs for power levels varying from 10 up to 170 W (1.3 up to 22.1 W/cm²) at the gravity-assisted orientation is compared in Figure 8. As the power input was applied, the temperatures increased until they reached a steady-state condition.

The square channel PHP, Figure 8a, started its operation at 40 W (5.2 W/cm²) with a slug flow pattern in a random direction, which is the characteristic flow of a PHP, shown by the temperature oscillations. From 50 W to 160 W (6.5 to 20.8 W/cm²), the temperature fluctuations reduced and the device achieved a more stable operation, which characterized an annular flow, resulting in the lowest thermal resistance. No dry-out was experienced.

Figure 8b shows that PHP-B, with grooves in the evaporator section, could anticipate the startup, which happened at 20 W (2.6 W/cm²), with an evaporator temperature of 30 °C. However, in this case, the device was operating as a heat pipe with an annular flow, as no temperature oscillations were observed. At 110 W (14.3 W/cm²), temperature fluctuations and a slight decrease in the evaporator temperatures showed the beginning of the PHP operation, in a slug flow pattern. Another flow modification was observed at 140 W (18.2 W/cm²), probably due to the transition again to the annular flow, which attained a better performance of the device. No dry-out was noticed.

For the PHP-C, Figure 8c shows that the entire grooved device showed a vapor front advancing to the condenser since the first heat load. At 30 W, the heat exchanger achieved a steady operation as a heat pipe. Temperature oscillations at 70 W (9.1 W/cm²) followed by a sudden drop in the evaporator temperature for a heat load of 80 W (10.4 W/cm²), characterized the activation of the device. In the sequence, the annular and stable flow was established until the evaporator dry-out at 130 W (16.9 W/cm²).

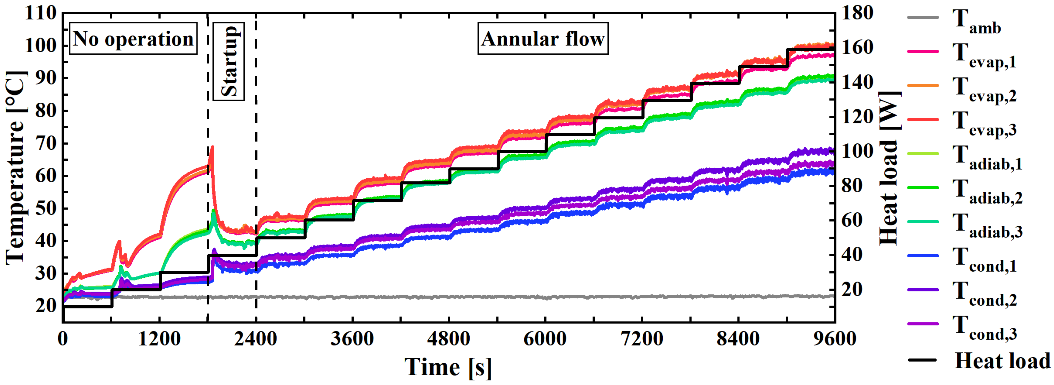


a) PHP-A (square channels) with 1.09 ml

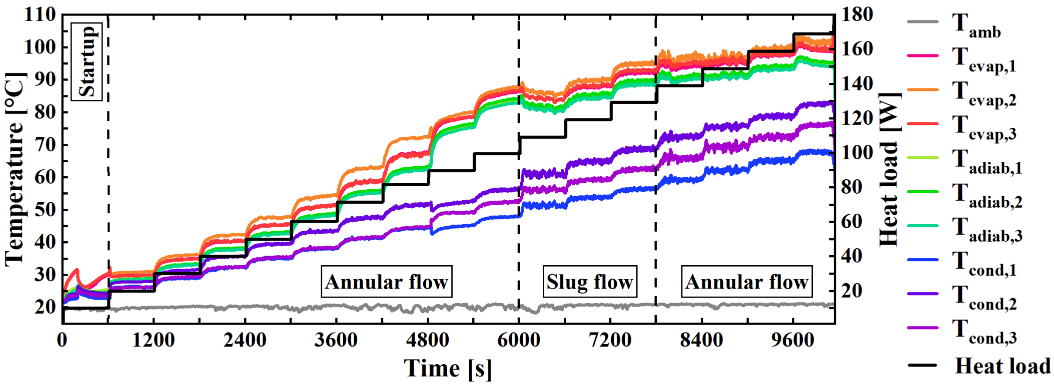


b) PHP-B (square channels with grooves in the evaporator) with 1.20 ml

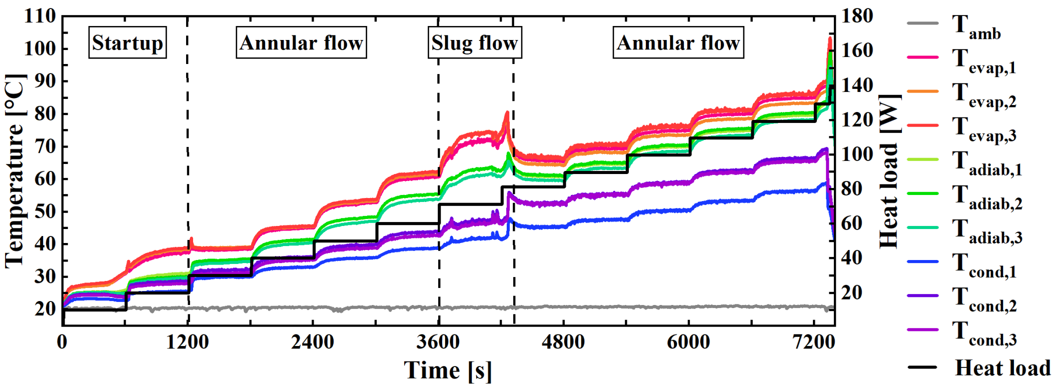


c) PHP-C (square channels with grooves in the entire length) with 1.50 ml

Figure 8. Transient behavior of PHPs at gravity-assisted orientation.

PHP transient behaviors in horizontal orientation are shown in Figure 9 under thermal loads between 10 and 140 W (1.3 and 18.2 W/cm²). As for the vertical position, a steady-state condition was reached for each power input. PHP-A with 1.60 ml (Figure 9a) presented a startup at 30 W and an evaporator temperature of proximately 65 °C. After that, the temperature oscillations and slug-plug flow continued until the annular flow was reached at 80 W (10.4 W/cm²). The test was finalized when the evaporator achieved 100 °C, without dry-out.

The PHP-B, with the grooves in the evaporator section and filled with the best volume of working fluid, was capable to initiated the oscillation motion at 40 W (5.2 W/cm²) and almost 90 °C in the evaporator section, as shown in Figure 9b. Without the gravity assistance, the heat pipe behavior was not accomplished, passing direct to a PHP operation at high temperature, i.e., slug flow pattern. Due to the higher temperatures and the limitation of 100 °C, the PHP worked with a maximum heat load of 60 W (7.8 W/cm²). No dry-out was noticed. In this position, the PHP with grooves over the entire channel (PHP-C) could not operate as a heat pipe or a pulsating heat pipe.

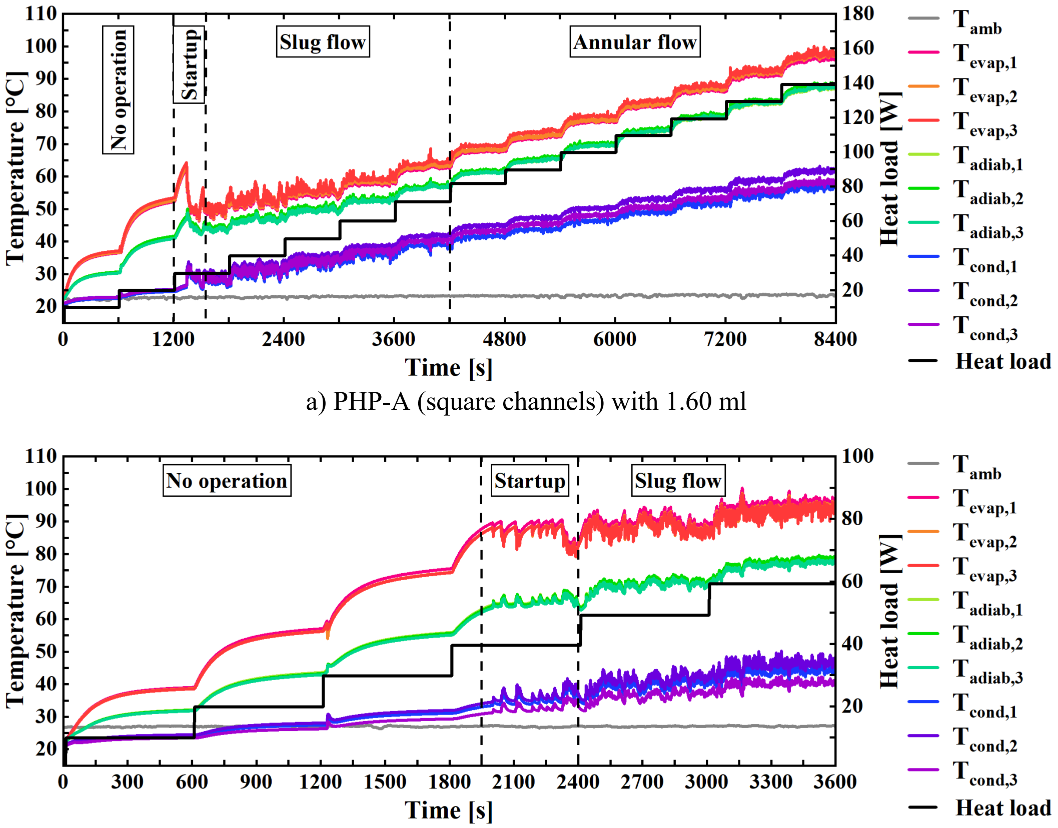


a) PHP-A (square channels) with 1.60 ml



b) PHP-B (square channels with grooves in the evaporator) with 1.50 ml

Figure 9. Transient behavior of PHPs at horizontal orientation.

To sum up, the 4 (four) machined grooves and the edges of the square channel worked as a capillary structure. With gravity's help, the grooves afforded behaviors analogous to the heat pipe for PHP-B and PHP-C under lower thermal loads, without large bubble formations, as the liquid is spread along the evaporator, starting earlier the operation than the PHP-A. Also, as the heat load improved, grooves assisted the slug-plug flow transition to an annular for better thermal performance. However, without the body force presence, the promoted capillarity was not able to overlap the pressure drops for a proper heat pipe function, i.e., the small size of grooves increased the liquid pressure drops, blocking the liquid motion. Besides, excess liquid was supplied to the evaporator, delaying the slug-plug flow of the PHP-B, and requiring a larger temperature difference to initiate the operation. Moreover, the extremely wet evaporator inhibits the oscillation motion in the PHP-C within the safe operating range.

Figure 10 presents the overall thermal resistance as a function of the heat load (and heat flux) of the proposed PHPs with the best configuration, i.e., the amount of liquid that provided the better thermal performance. Figure 10a and 10b illustrate the thermal resistance operating in gravity-assisted and horizontal orientations, respectively. The startup can be observed by the sudden decreases in the thermal resistance. As already mentioned, the conduction thermal resistance of the PHPs was equal to 1.40 ± 0.23 ºC/W.

In the gravity-assisted operation mode, all the PHPs worked satisfactorily. After the activation, the PHP-A worked successfully and with a similar thermal resistance for all the tested thermal loads, reaching a minimum of 0.24 ± 0.02 °C/W. The evaporator grooves afforded the PHP-B the early startup and the lowest thermal resistance, even in the low power inputs. Besides a slight increase in the value during the flow pattern change, the maximum thermal resistance was 0.27 ± 0.03 °C/W. The best thermal performance showed a minimum thermal resistance of 0.15 ± 0.02 ºC/W, which corresponds to about 11% of the only conduction thermal resistance, at 170 W (22 W/cm²). PHP-C had a more anticipate startup than the square channel PHP. Between the startup and the flow pattern modification (30 and 80 W), the PHP-C with grooves entirely presented a higher thermal resistance. However, from 80 up to 120 W, grooves enhanced the heat transfer mechanism and reduced to 0.18 ± 0.02 °C/W the thermal resistance.

Figure 10b shows the thermal resistance comparison in horizontal orientation. In this situation, the unique device able to operate without gravity assistance, for a large heat transfer power range, from 30 to 140 W (3.9 to 18.2 W/cm²), was the PHP with square channels, PHP-A. PHP-B started at 40 W (5.2 W/cm²), operating until 60 W, when achieved its lowest thermal resistance, 0.85 ± 0.11 °C/W. The PHP-C thermal resistance remained approximately at the empty PHP level, showing that it did not work.

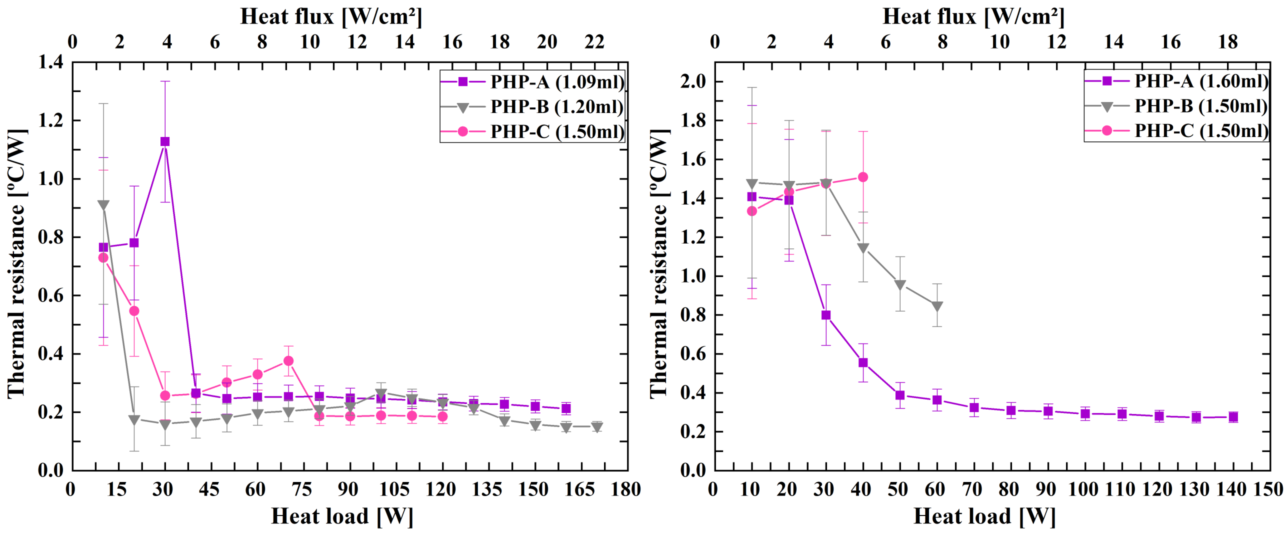


a) gravity-assisted orientation

b) horizontal orientation

Figure 10. Thermal resistance comparison between PHP-A, PHP-B and PHP-C.

From the comparison, it can be concluded that the grooves in the evaporator of a PHP improved its heat transfer capacity by anticipating the operation startup, reducing the thermal resistance, and supporting a higher heat flux when the condenser is above the evaporator. However, the conventional square channel showed the best thermal behavior in the horizontal position. As a result, the new channel design in the evaporator showed to be a better alternative for electronics cooling in a gravity-assisted orientation, especially if a wide range of dissipated power needs to be covered. Also, the traditional square channels are the best option for narrow spaces under concentrated thermal loads in the horizontal orientation.

## 5. CONCLUSIONS

The impact of grooves on the heat transfer performance of mini flat pulsating heat pipes with 16 parallel channels was experimentally investigated. Due to their size and geometry, these devices can be used for electronic cooling applications. A novel channel design, made of a square channel with 4 (four) machined grooves along the longitudinal direction, was proposed, combining characteristics of an oscillating heat pipe and capillary structure. The novel channel profile was used in two devices, PHP-B and PHP-C. Their essential difference was that PHP-C had grooves through all sections while PHP-B presented the novel design only in the evaporator section. Also, a conventional square channel pulsating heat pipe (PHP-A) was manufactured and its performance was used for comparison with the new grooved geometry proposed.

The thermal analysis showed that both PHPs with the novel channel (PHP-B and PHP-C) reduced the thermal resistance and anticipated the startup in the gravity-assisted orientation, over the whole range of investigated thermal loads. However, only the device with a square channel, PHP-A, operated satisfactorily without gravity assistance. Although the four machined grooves and the edges of the square channel worked as a capillary structure, the promoted capillarity was not enough for a proper operation in the horizontal position. Besides, excess liquid was supplied to the evaporator, delaying the slug-plug flow of the PHP-B and inhibiting the oscillation motion in the PHP-C within the safe operating range.

As the main result, the new channel design in the evaporator showed to be a better alternative for electronics cooling in a gravity-assisted orientation, especially if a wide range of dissipated power needs to be covered. Moreover, the traditional square channels are the best option for narrow spaces under concentrated thermal loads in the horizontal orientation.

## 6. ACKNOWLEDGEMENTS

The authors acknowledge CNPq (Conselho Nacional de Desenvolvimento Científico e Tecnológico) for providing financial support (grant numbers 149892/2019-5 and 423968/2018-1) to the present research.

## 7. REFERENCES

Baturkin, V., 2005. Micro-satellites thermal control - Concepts and components. *Acta Astronautica*, Vol. 56, pp. 161–170.

Cai, Q., Chen, C.L., Asfia, J.F., 2006. Heat transfer enhancement of planar pulsating heat pipe device, in: Proceedings of 2006 ASME International Mechanical Engineering Congress and Exposition, IMECE2006 - Heat Transfer. American Society of Mechanical Engineers (ASME), Chicago, IL, United States.

Cisterna, L.H.R., Vitto, G., Cardoso, M.C.K., Fronza, E.L., Mantelli, M.B.H., Milanez, F.H., 2020. Charging procedures: effects on high temperature sodium thermosyphon performance. *Journal of the Brazilian Society of Mechanical Sciences and Engineering*, Vol. 42, pp. 1–11.

Holman, J.P., 2011. Experimental methods for engineers, 8th ed, McGraw-Hill. New York, USA.

Khandekar, S., Charoensawan, P., Groll, M., Terdtoon, P., 2003. Closed loop pulsating heat pipes - Part B: Visualization and semi-empirical modeling. *Applied Thermal Engineering*, Vol. 23, pp. 2021–2033.

Krambeck, L., Domiciano, K.G., Betancur-arboleda, L.A., Mantelli, M.B.H., 2022. Novel flat plate pulsating heat pipe with ultra sharp grooves. *Applied Thermal Engineering*, Vol. 211, pp. 118509.

Laun, F.F., Lu, H., Ma, H.B., 2015. An experimental investigation of an oscillating heat pipe heat spreader. *Journal of Thermal Science and Engineering Applications*, Vol. 7, pp. 021005.

Mameli, M., Araneo, L., Filippeschi, S., Marelli, L., Testa, R., Marengo, M., 2014. Thermal response of a closed loop pulsating heat pipe under a varying gravity force. *International Journal of Thermal Sciences*, Vol. 80, pp. 11–22.

Qu, J., Li, X., Xu, Q., Wang, Q., 2017. Thermal performance comparison of oscillating heat pipes with and without helical micro-grooves. *Heat and Mass Transfer/Waerme- und Stoffuebertragung*, Vol. 53, pp. 3383–3390.

Qu, W., Zhou, Y., Li, Y., Ma, T., 2007. Experimental study on mini pulsating heat pipes with square and regular triangle capillaries, in: 14th International Heat Pipe Conference (IHPC). Florianopolis, Brazil.

Taft, B.S., Williams, A.D., Drolen, B.L., 2012. Review of pulsating heat pipe working fluid selection. *Journal of Thermophysics and Heat Transfer*, Vol. 26, pp. 651–656.

Winkler, M., Rapp, D., Mahlke, A., Zunftmeister, F., Vergez, M., Wischerhoff, E., Clade, J., Bartholomé, K., Schäfer-Welsen, O., 2020. Small-sized pulsating heat pipes/oscillating heat pipes with low thermal resistance and high heat transport capability. *Energies*, Vol. 13.

Yang, H., Khandekar, S., Groll, M., 2009. Performance characteristics of pulsating heat pipes as integral thermal spreaders. *International Journal of Thermal Sciences*, Vol. 48, pp. 815–824.

Zhang, Y., Faghri, A., 2008. Advances and unsolved issues in pulsating heat pipes. *Heat Transfer Engineering*, Vol. 29, pp. 20–44.

## 8. RESPONSIBILITY NOTICE

The authors are the only responsible for the printed material included in this paper.